

Full Length Research Paper

Sintering characteristics of ceramsite manufactured from blast furnace slag and sewage sludge

Zhulai Wang

¹School of Civil Engineering, Nanjing Forestry University, Nanjing, Jiangsu Province 210037, China.

²College of Environment, Hohai University, Nanjing, Jiangsu Province 210024, China.

E-mail: wangzhulai66@yahoo.com or wangzhulai@126.com. Tel: +86-025-85427691.

Accepted 23 December, 2011

To develop a method of recycling solid wastes, blast furnace slag (BFS) and sewage sludge (SS) were added as components for making ceramsite. This study examined the sintering characteristics of ceramsite at different sintering temperatures and duration and different mass ratios of materials (BFS:SS:clay). The results show that as the sintering temperature and duration increased, the pore-size diameter gradually increased, reaching a maximum of 120 nm at 1100°C for 20 min. The turning point for the pore-size diameter was at 1050°C for 20 min. In keeping with the variation in pore-size diameter, the highest and lowest porosity of the ceramsite reached 88 and 62%, respectively. The different mass ratios of three raw materials (BFS, SS and clay) had no significant effect on the thermal behaviors of the ceramsite, with the DT-TG analysis curves showing essentially the same trends in terms of variation. As the sintering temperature increased, the complex crystalline phases appeared at 900°C, while no variation occurred within the main crystalline phases except for the transformation from akermanite ($\text{Ca}_2\text{MgSi}_2\text{O}_7$) to gehlenite [$\text{Ca}_2\text{Al}(\text{AlSiO}_7)$] at 1050°C.

Key words: Ceramsite, blast furnace slag, sewage sludge, sintering characteristics.

INTRODUCTION

With the rapid economic growth of modern society, solid wastes as by-products of industry, households and agriculture are increasingly produced every year around the world. In view of the development of regenerative resources, research on the management and recycling of solid wastes, especially industrial solid wastes have been conducted in many countries and regions (Duan et al., 2008; Lu et al., 2006; Alexandre et al., 2006; Mohan et al., 2006).

Blast furnace slag (BFS) contains mainly inorganic constituents such as silica (30 to 35%), calcium oxide (28 to 35%), magnesium oxide (1 to 6%) and $\text{Al}_2\text{O}_3/\text{Fe}_2\text{O}_3$ (18 to 258%) (Das et al., 2007). Because of its simple components, studies on the recycling of BFS have been

conducted in many fields including sorbents, packing or producing ceramsite combined with other solid wastes.

BFS can be used as sorbents of phosphate for water solutions. The kinetic measurements of adsorption confirmed that the sorption of phosphorus on crystalline as well as amorphous slags can be described by a model involving pseudo-second-order reaction, and that the phosphorus sorption followed the Langmuir adsorption isotherm (Kostura et al., 2005). BFS samples have been compared with natural eelgrass sediment (NES) in terms of its physicochemical characteristics, and researchers have also investigated the growth of eelgrass both in BFS and NES (Amelia et al., 2009). Steelworks slag can be blended with municipal sewage sludge to make ceramic specimens, which are then sintered in air using a muffle furnace and characterized by density, strength, hardness, fracture toughness measurements, X-ray diffraction and SEM investigations (Favoni et al., 2005).

Sewage sludge (SS) is one of the final products in the

Abbreviations: BFS, Blast furnace slag; SS, sewage sludge.

Table 1. Elements analyses.

Element	Si	Ca	Al	Mg	Fe	K	Na	P	Sb
BFS (w-%)	10.06	19.05	6.20	3.78	0.77	0.59	0.31	0.13	4.26
SS (w-%)	9.24	1.39	2.97	0.53	3.68	1.48	0.22	0.33	0.42
Clay (w-%)	16.68	0.69	6.28	0.78	3.19	0.99	0.63	0.05	-
Element	Mo	Sn	Ti	Mn	Cd	Se	Pd	O	C
BFS (w-%)	1.94	1.94	0.56	0.16	0.02	-	-	45.48	4.75
SS (w-%)	1.09	1.64	0.32	0.07	-	0.10	0.09	30.69	45.69
Clay (w-%)	0.07	1.10	0.33	-	-	-	-	52.08	17.13

Table 2. Samples contents and ratios.

Type of ceramite	BFS (w-%)	SS (w-%)	Clay (w-%)
SSA	0	70	30
SSB	10	60	30
SSC	20	50	30

BFS, Blast furnace slag; SS, sewage sludge.

treatment of sewage at wastewater treatment plants. It usually contains high levels (10 to 20% or more) of organic matter, and it is rich in the nitrogen and phosphorus that are essential for plant growth (Cheng et al., 2007). Owing to its characteristics, SS can be used to produce just ceramsite alone or it can be blended with other solid wastes. Sintering temperature had a significant effect on the characteristics of sludge ceramsite, and it was found that 1000°C was the optimal sintering temperature (Wang et al., 2008; Xu et al., 2008). Wastewater sludge and drinking-water sludge could be mixed for making ceramsite. The compounds Fe_2O_3 , CaO , MgO , SiO_2 and Al_2O_3 are the major basic oxides in these sludges. The optimal contents of Fe_2O_3 , CaO and MgO ranged from 5 to 8%, 2.75 to 7% and 1.6 to 4%, respectively, and the optimal ratios of ($\text{Fe}_2\text{O}_3+\text{CaO}+\text{MgO}$) to ($\text{SiO}_2+\text{Al}_2\text{O}_3$) ranged from 0.175 to 0.45 (Zou et al., 2009; Xu et al., 2009). Dry sewage sludge (DSS) can be also blended with coal ash (CA) to produce a lightweight aggregate. Using DSS enhanced the pyrolysis–volatilization reaction due to its high organic matter content, while decreasing the bulk density and sintering temperature. Adding CA improved the sintering temperature while effectively decreasing the pore size and increasing the compressive strength of the product (Wang et al., 2009).

The objective of this study was to evaluate the feasibility of blending BFS with SS to manufacture ceramsite and characterizing the variation of its pore structures, thermal behaviors and crystalline phases at different temperatures and sintering duration.

MATERIALS AND METHODS

The BFS in this study was obtained from the first energy factory of the MA STEEL group, which is located in Ma'anshan city, China. The factory produces BFS by water quick-cooling during the process of steelmaking in a blast furnace. SS was produced from a dewatering workshop of Jiangxinzhou Wastewater Treatment Plant located in Nanjing city, China. In this plant, a primary sedimentation basin, A/O and a secondary sedimentation basin are the major wastewater treatment technologies, and the sludge dewatered by pressure filter came from the excess sludge of the secondary sedimentation basin. In addition, clay was obtained from the worksite of the 3rd Bridge of Yangtze River, Nanjing, China, and the plasticity index of clay was greater than 17. The chemical compositions of three raw materials mentioned above are shown in Table 1.

The raw materials were ground with a SF-130C pulverizer (ZhongCheng Pharmaceutical Factory, JiShou City, China) at sizes below 100 mm to ensure thorough mixing. Three different dry weight ratios of slag:sludge:clay were evaluated in this experiment and the ratios are given in Table 2. The ratios were identified as SSA, SSB and SSC.

Experimental procedures

The raw materials were mixed and a DZ-60 pelletizing machine (ZhongCheng Pharmaceutical Factory, Jishou City, China) was used to pelletize the ceramsite to particle sizes of 4 to 6 mm and the samples were left in a room at a temperature of about 20°C for 4 days. The samples were then dried at 105°C in a drying oven for 24 h. The samples subjected to DT-TG analyses (all three types) were not preheated or sintered, while the sample used to examine pore-diameter structure and to analyze the crystalline phase's analyses, namely SSC, was first preheated at 400°C for 20 min and then sintered at varying temperatures and duration. The chemical

compositions of the raw materials were determined by electron energy disperse spectroscopy (INCA 250 EDS, UK). The examination of pore-diameter structure was conducted by mercury porosimeter (AutoPore 9510, US) at a low pressure of 30 psi and a high pressure of 60,000 psi. The thermal behavior of the products was examined by a simultaneous DT-TG analyses instrument (Diamond TG/DTA, US) when the samples were heated at a rate of 10°C/min from 30 to 1100°C in air. The crystalline phases of the ceramsite were measured by x-ray diffractometer (D/max-2500/PC, Japan) with 50 mA and 40 kV.

RESULTS AND DISCUSSION

Effect of sintering temperature and duration on pore-diameter structures of ceramsite

In order to examine the effect of sintering temperatures and duration on the pore-diameter structure of the ceramsite, the SSC sample was sintered at temperatures of 900, 1000, 1050 and 1100°C, and at durations of 10 and 20 min after an initial preheating at 400°C for 20 min. The results are shown in Figure 1 and Table 3. It can be seen from Figure 1 that small pores below 20 nm were the major pore structure up to 1050°C for 10 min. Larger pores with diameters over 20 nm were evident at 900°C, 10 min and 900°C at 20 min, varying from 20 to 100 nm up to 1050°C, 10 min. The major pore structure continued to increase in size, reaching a final consistent range between 40 and 160 nm at 1100°C for 20 min. In general therefore, the pore diameter gradually increased as the sintering temperatures increased and as the sintering duration varied from 10 to 20 min. The explanation of this phenomenon was that owing to the decomposition of organic matters producing CO₂, CO and C as the deoxidizer of Fe₂O₃ to form CO₂, many small and large pores appeared simultaneously in the ceramsite before 900°C. From 1000°C, the small pores started melting to form larger pores under the influence of fluxing agents, such as Fe₂O₃, CaO and MgO, and the glass phases were finally produced resulting in the increasing of the compressive strength of ceramsite.

The porosity of ceramsite is a ratio of the volume of the inner pores to the total volume of the particles of the ceramsite. Table 3 shows the variation of the ceramsite porosity at different sintering temperatures and duration. The highest porosity was 88%, which appeared at 900°C, 10 min and 62% was the lowest porosity, which appeared at 1050°C, 20 min. The low peak of porosity was shown twice at 1000°C, 20 min and 1050°C, 20 min, respectively. The first peak of 64% was due to the decrease in the number of small pores, which was obtained from the release of CO₂ and CO. The melting of big pores and the forming of glass phases were the reasons for the appearance of the second peak of 62%.

DT-TG analyses

To examine the effect of different mass ratios of the three

raw materials on the thermal behaviors of the ceramsite, the SSA, SSB and SSC samples heated from 30 to 1100°C in air were tested by DT-TG analysis. The results are shown in Figure 2a to c.

The DT-TG curves for the three samples show basically the same variation except for a negligible difference from 800 to 1000°C in Figure 2b and c, in which there was an endothermic change and a 6% weight loss at temperatures between 30 and 225°C; an exothermic change and 4% weight loss at temperatures between 225 and 390°C; a significant endothermic change with 6% weight loss at temperatures between 390 and 750°C; and finally at 1000°C and higher there was an endothermic change and minimal weight loss. In general, the weight loss gradually decreased in the samples from SSA to SSC, finally reaching a minimum in SSC. This phenomenon can be explained as a result of the evaporation of adsorbed water molecules happening below 225°C; a H₂O loss from the ceramsite mixture between 225 and 390°C; the decomposition between 390 and 750°C of the carbonous materials were decomposed to release many gases such as CO₂, CO, and so on; the formation of crystalline phases and some phases changes appearing after 900°C; a gradual decrease in the content of SS from SSA to SSC; and a reduction in the ignition loss. The two small valleys that occurred between 800 and 1000°C shown in Figure 2b and c were due to the dehydration of silicate hydrates (Xu et al., 2008).

Crystalline phases and chemical composition analyses

To evaluate the effect of different sintering temperatures on the variation of crystalline phases, the SSE sample were divided into four parts of equal quality and sintered at 900, 1000, 1050 and 1100°C, respectively under the same duration of 20 min. The results are shown in Table 4 and Figure 3.

It can be observed from Table 4 and Figure 3 that the major crystalline phases at 900 to 1100°C were quartz (SiO₂), akermanite (Ca₂MgSi₂O₇), albite (NaAlSi₃O₈) and hematite (Fe₂O₃). The major crystalline phases at 1050 to 1100°C were quartz (SiO₂), albite (NaAlSi₃O₈), gehlenite [Ca₂Al(AlSiO₇)] and hematite (Fe₂O₃); the only crystalline transformation was from akermanite (Ca₂MgSi₂O₇) to gehlenite [Ca₂Al(AlSiO₇)]; hematite (Fe₂O₃) was consistently present between 900 and 1100°C and it did not react with other constituents in the sample to form a crystalline phase. The crystalline phase of akermanite (Ca₂MgSi₂O₇), appearing at 900°C, indicated that owing to the fact that it contained a significant amount of organic matters (SS), the formation of crystals happened before 900°C and the melting point of ceramsite manufactured from BFS, SS, and clay was less than that of products produced from clay only, which was up to 1300°C. The additional liquid phases led to the formation

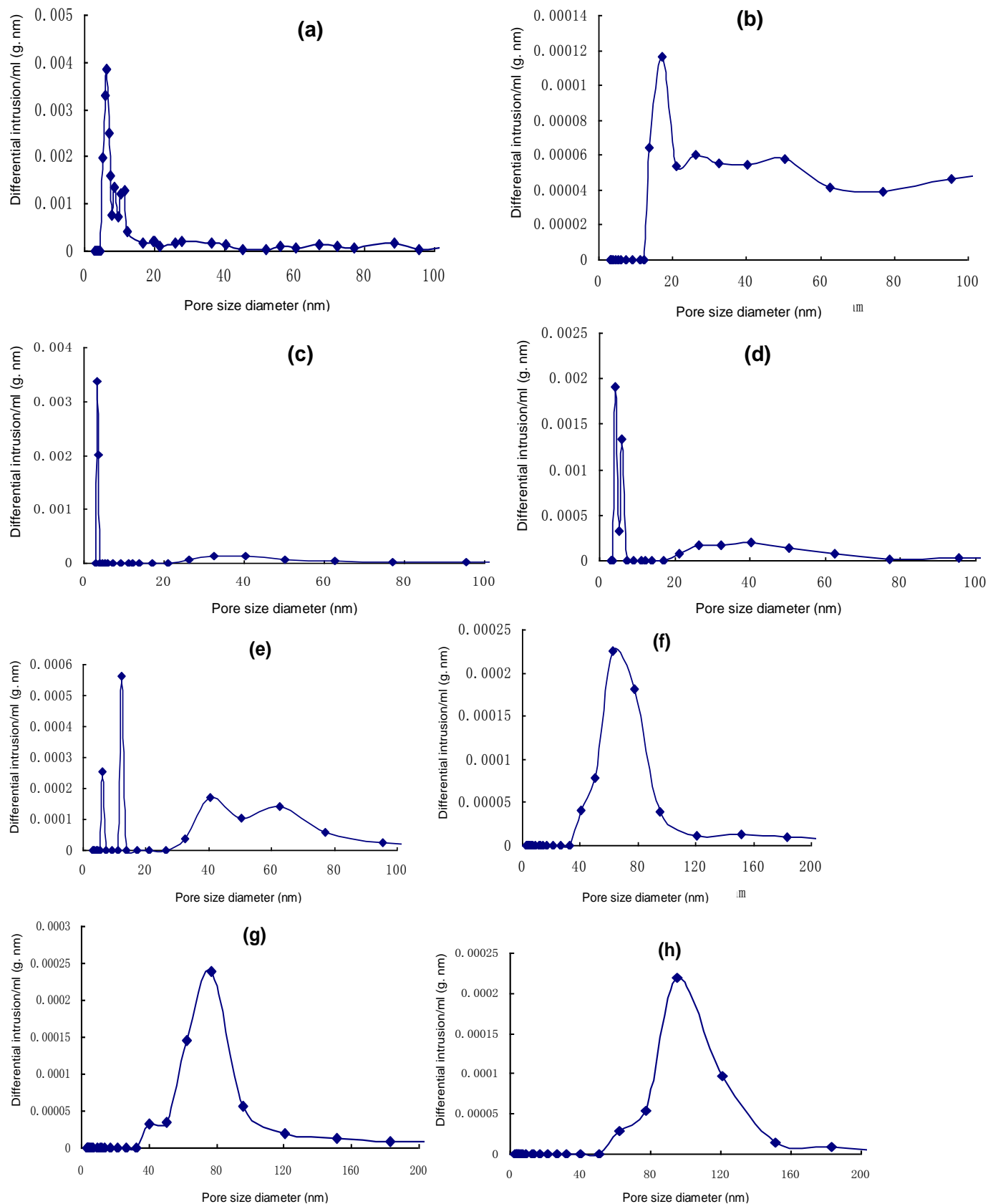
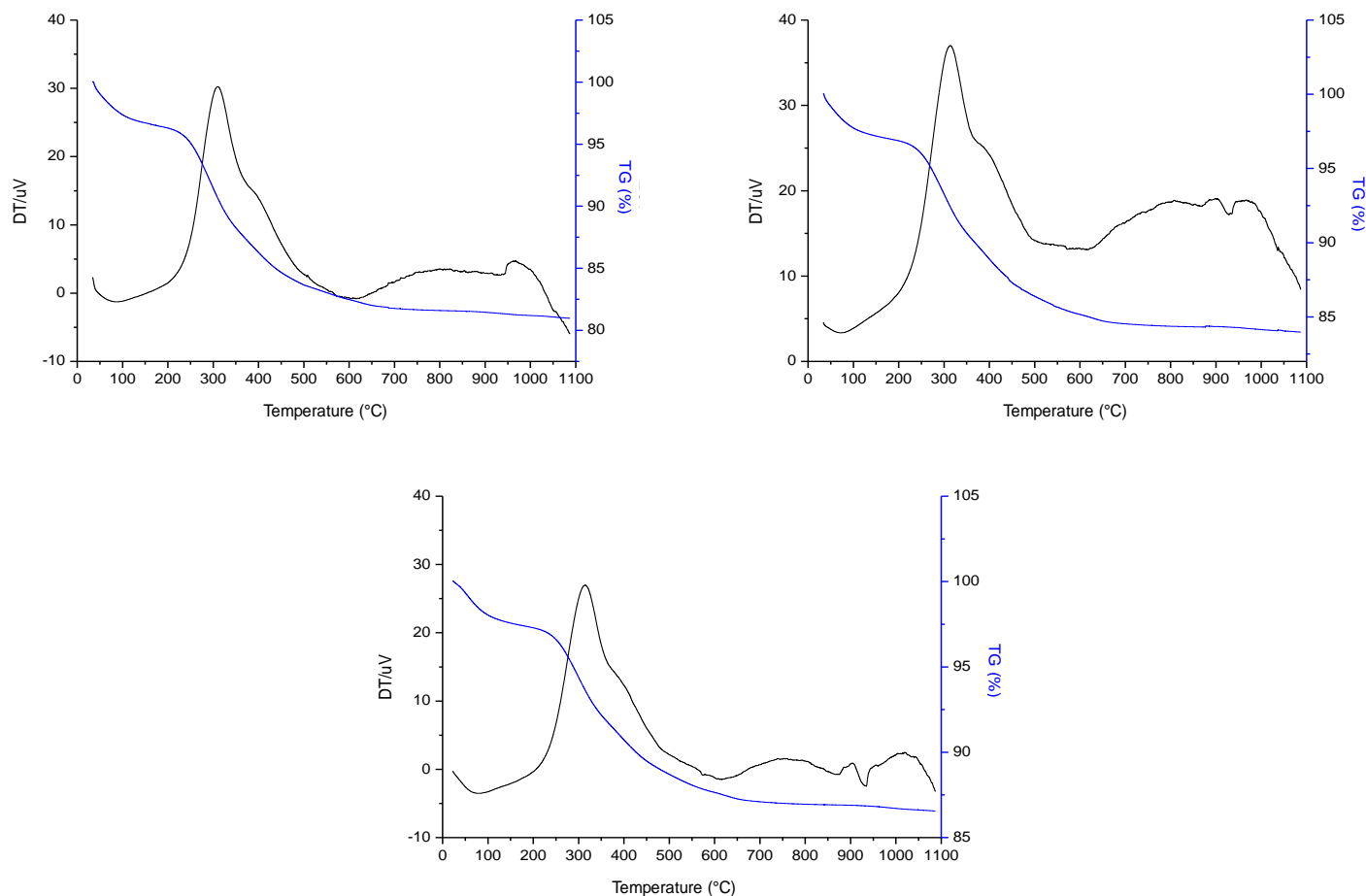


Figure 1. Variation of pore-diameter structure of ceramsite sintered at different temperatures and duration. (a) 900°C at 10 min; (b) 900°C at 20 min; (c) 1000°C at 10 min; (d) 1000°C at 20 min; (e) 1050°C at 10 min; (f) 1050°C at 20 min; (g) 1100°C at 10 min; (h) 1100°C at 20 min.

Table 3. Porosity variation as a function of different sintering methods.

Sintering method		Porosity (%)
900°C	10 min	88
	20 min	78
1000°C	10 min	64
	20 min	70
1050°C	10 min	77
	20 min	62
1100°C	10 min	63
	20 min	75

**Figure 2.** DT-TG analyses of (a) SSA; (b) SSB and (c) SSC.

of more complex crystalline phases, which was thought to correspond to the endothermic changes above 900°C in the DT curves in Figure 2. Meanwhile, the variation in crystalline phases above 1050°C was in accordance with the variation in pore-size diameters of ceramsite as

mentioned earlier, and as the sintering temperature increased, the complicated crystals gradually formed and the pore-size diameter increased. The main reactions of the transformation of crystalline phases in ceramsite might be as follows:

Table 4. Crystalline phases at different sintering temperatures.

Sintering temperature (°C)	Major constituent
900	Silicon oxide (SiO ₂)
	Akermanite (Ca ₂ MgSi ₂ O ₇)
	Albite (NaAlSi ₃ O ₈)
	Hematite (Fe ₂ O ₃)
1000	Silicon oxide(SiO ₂)
	Akermanite(Ca ₂ MgSi ₂ O ₇)
	Hematite (Fe ₂ O ₃)
	Albite (NaAlSi ₃ O ₈)
1050	Quartz (SiO ₂)
	Albite (NaAlSi ₃ O ₈)
	Gehlenite (Ca ₂ Al(AlSiO ₇))
	Hematite (Fe ₂ O ₃)
1100	Quartz (SiO ₂)
	Albite (NaAlSi ₃ O ₈)
	Gehlenite (Ca ₂ Al(AlSiO ₇))
	Hematite (Fe ₂ O ₃)

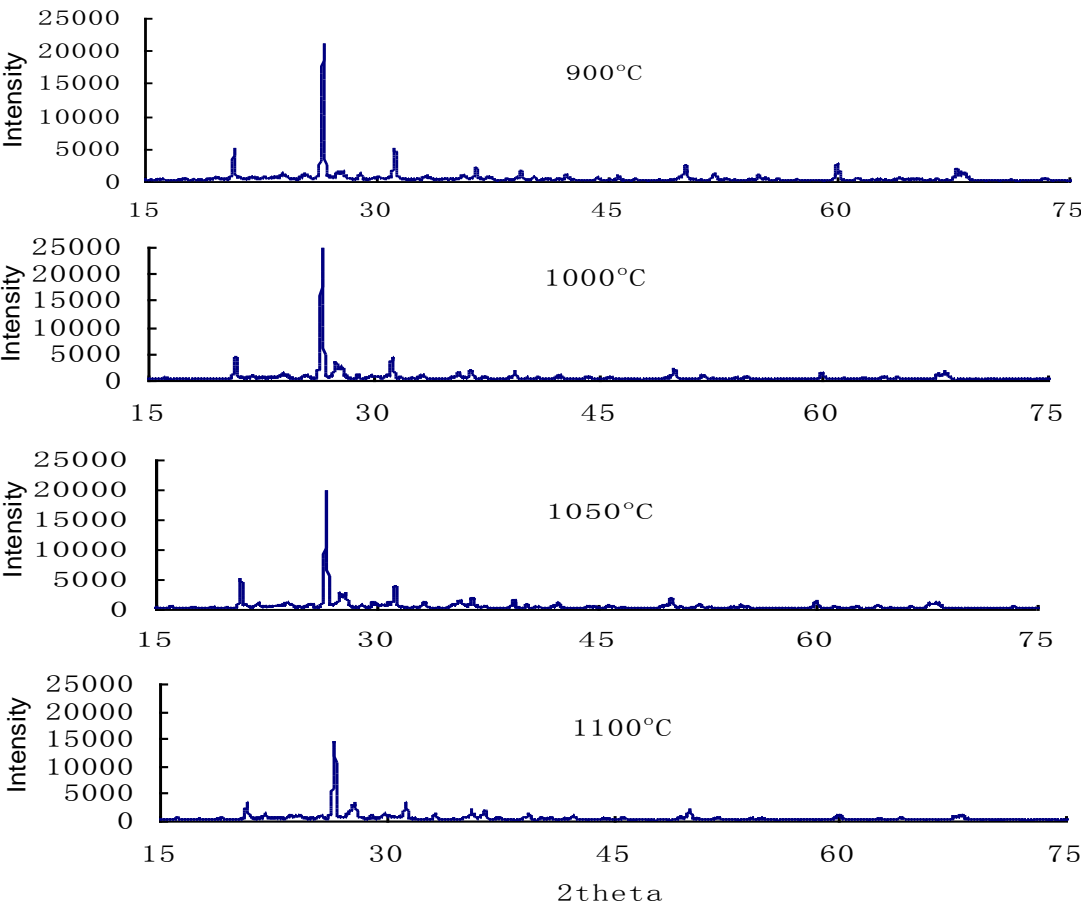
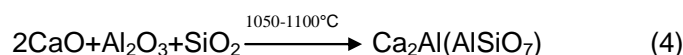
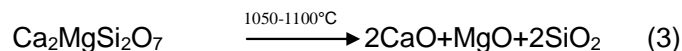
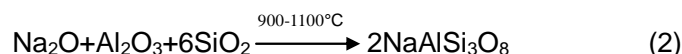
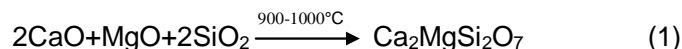


Figure 3. X-ray diffraction of SSE at 900 to 1100°C for 20 min.



Conclusion

Based on the results obtained in this study, the following conclusions were drawn:

(1) As the sintering temperature and duration increase, the pore-size diameter gradually increases up to the maximum of 120 nm at 1100°C, 20 min and the turning point of the pore-size diameter was at 1050°C, 20 min. Corresponding to the variation of the pore size diameter, the highest porosity of ceramsite reached 88% while 62% was the lowest porosity of the ceramite.

(2) The effect of the different mass ratios of the three raw materials on the thermal behavior of ceramsite was very minimal and the DT-TG analysis curves exhibited essentially the same trends in variation.

(3) As the sintering temperature increased, complex crystalline phases appeared at 900°C and no variation occurred on the main crystalline phases except for the transformation from akermanite ($\text{Ca}_2\text{MgSi}_2\text{O}_7$) to gehlenite [$\text{Ca}_2\text{Al}(\text{AlSiO}_7)$] at 1050°C.

ACKNOWLEDGEMENT

A Project Funded by the Priority Academic Program Development of Jiangsu Higher Education Institutions, China.

REFERENCES

- Alexandre M, Filipe D, Viriato S (2006). Municipal solid waste disposal in Portugal. *Waste Manage.*, 26: 1477-1489.
- Amelia BH-F, Nakano Y, Nakai S, Nishijima W, Okada M (2009). Evaluation of blast furnace slag as basal media for eelgrass bed. *J. Hazard. Mater.*, 166: 1560-1566.
- Das B, Prakash S, Reddy PSR, Misra VN (2007). An overview of utilization of slag and sludge from steel industries. *Resour. Conserv. Recy.*, 50: 40-57.
- Kostura B, Kulveitova H, Lesko J (2005). Blast furnace slags as sorbents of phosphate from water solutions. *Water Res.*, 39: 1795-1802.
- Favoni C, Minichelli D, Tubaro F, Bruckner S, Bachiarrini A, Maschio S (2005). Ceramic processing of municipal sewage sludge(MSS)and steelworks slags(SS). *Ceram. Int.*, 31: 697-702.
- Xu GR, Zou JL, Li GB (2008). Effect of sintering temperature on the characteristics of sludge ceramsite. *J. Hazard. Mater.*, 150: 394-400.
- Xu GR, Zou JL, Li GB (2009). Ceramsite obtained from water and wastewater sludge and its characteristics affected by ($\text{Fe}_2\text{O}_3 + \text{CaO} + \text{MgO}$)/($\text{SiO}_2 + \text{Al}_2\text{O}_3$). *Water Res.*, 43: 2885-2893.
- Cheng H, Xu W, Liu J, Zhao Q, He Y, Chen G (2007). Application of composted sewage sludge (CSS) as a soil amendment for turfgrass growth. *Ecol. Eng.*, 29: 96-104.
- Duan H, Huang Q, Wang Q, Zhou B, Li J (2008). Hazardous waste generation and management in China: A review. *J. Hazard. Mater.*, 158: 221-227.
- Zou JL, Xu GR, Li GB (2009). Ceramsite obtained from water and wastewater sludge and its characteristics affected by Fe_2O_3 , CaO , and MgO . *J. Hazard. Mater.*, 165: 995-1001.
- Lu L-T, Hsiao T-Y, Shang N-C, Yu Y-H, Ma H-W (2006). MSW management for waste minimization in Taiwan: The last two decades. *Waste Manage.*, 26: 661-667.
- Mohan R, Spiby J, Leonardi GS, Robins A, Jefferis S (2006). Sustainable waste management in the UK: The public health role. *Public Health*, 120: 908-914.
- Wang X, Jin Y, Nie Y, Huang Q, Wang Q (2009). Development of lightweight aggregate from dry sewage sludge and coal ash. *Waste Manage.*, 29: 1330-1335.
- Wang X, Jin Y, Wang Z, Mahar RB, Nie Y (2008). A research on sintering characteristics and mechanisms of dried sewage sludge. *J. Hazard. Mater.*, 160: 489-494.